Progress In Electromagnetics Research Letters, Vol. 105, 57–62, 2022

Design of High-Selective Wideband Bandpass Filter with a Notched-Band and Harmonic Suppression

Jie Liu, Yun Xiu Wang*, Guang Yong Wei, Rui Lin Jia, and Yin Long Duan

Abstract—A high-selective wideband bandpass filter (BPF) with a notched-band and harmonic suppression is proposed in this paper. Firstly, a uniform impedance resonator with an embedded open-circuited stub square loop is applied in the filter design. By adopting parallel-coupling structure at I/O ports, such a resonator can generate a notched-band within the passband due to the counter-phase cancellation of two dissimilar signal paths. The width of the square loop can be adjusted to select the location of the notched-band. Secondly, by introducing an L-shaped open-circuited stub to one input feed line, a transmission zero (TZ) is created. It can be used to suppress higher harmonic passband. The filter is designed and fabricated with the notched-band centered at 8.1 GHz, and two TZs are implemented at the both sides of the passband. Simulated and measured results show that the filter has a good selectivity and a wider stopband characteristic.

1. INTRODUCTION

Due to the characteristics of simple system structure, high transmission rate, low power consumption, and high concealment, wide- or even ultra-wideband (UWB) technology has prospective applications in the fields of communication, radar, position, etc. As one of the essential components of UWB systems, UWB bandpass filter (BPF) has a great impact on the system. Low insertion loss, wide rejection stopband, sharp roll-off in close proximity to the passband are several basic demands in filter design. Up to now, common design techniques include cascading a low-pass filter and a high-pass filter, multi-mode resonators (MMRs), defected ground structure (DGS), multilayer coupling structure, etc. Among them, one simple and effective method to realize wideband BPFs is to connect a lowpass filter and a highpass filter in series [1]. But one obvious flaw of the method is its large size. MMRs have been widely applied to design wideband BPFs [2–4]. In another paper [5], a compact BPF is developed using a stub-tapped half-wavelength transmission line resonator, which can improve the performance of the filter by generating two TZs. But these filters have narrow upper stopband rejection performance. The added defected ground structure (DGS) to a BPF can improve the out of band rejection property of the filter without increasing the overall dimensions. But in some cases the in-band frequency response of the filter is affected too [6]. Although multi-layer coupling can realize UWB filter, its structure and design are relatively complex [7–9]. To suppress some harmful interferences within the wideband spectrum, we should introduce a single or multiple notched-bands [10–13]. In [10], a redial stub loaded resonator with a defected microstrip structure is used to provide two notched bands. In another paper [11], to obtain multiple freely adjustable notched-bands, the authors proposed an E-shaped MMR etched with parallel defected microstrip structures.

In this letter, a wideband BPF with a notched-band and harmonic suppression is realized by using a square ring loaded with an open stub. The characteristics of the proposed filter are illustrated by means of even- and odd-mode method. To suppress the parasitic passband, an open-circuited stub is

Received 10 May 2022, Accepted 24 June 2022, Scheduled 19 July 2022
* Corresponding author: Yun Xiu Wang (627662147@qq.com).
The authors are with the School of Electronic Information Engineering, China West Normal University, Nanchong 637009, China.

connected to one feed line. Finally, the presented filter is designed and measured on a substrate with $\varepsilon_r = 9.6$, thickness $= 0.8$ mm and loss tangent $\tan\delta = 0.001$. A filter prototype is designed, fabricated, and measured. Both simulation and measurement results are provided to verify the filter performance.

2. THEORETICAL ANALYSIS

As depicted in Fig. 1(a), a square ring with an open-circuit stub loaded is connected to a uniform impedance microstrip line with respect to its center. Such a structure provides two signal transmission paths, path I along the horizontal line of L_3 and path II of the main signal path along S. Path I can be controlled by changing the length of L_2 and L_3. Odd-even mode analysis can be used to analyze the characteristics of the resonator because of its symmetric structure. When even mode excitation is applied, the central symmetry plane of this resonator is regarded as an ideal magnetic wall, and its equivalent circuit diagram can be shown in Fig. 1(b). The even-mode resonant frequency can be derived as

$$f_{\text{even}} \approx \frac{nc}{2\left(L_1 + L_2 + L_3/2 + L_4\right)\sqrt{\varepsilon_{re}}} \tag{1}$$

where c is the light speed in free space, $n = 1, 2, 3, \ldots$, and ε_{re} is the effective dielectric constant of the used substrate. Similarly, the equivalent circuit under odd mode excitation is demonstrated in Fig. 1(c). Hence, the odd-mode resonant frequency can be derived as

$$f_{\text{odd}} \approx \frac{(2n-1)\,c}{2\left(L_1 + L_3/2\right)\sqrt{\varepsilon_{re}}} \tag{2}$$

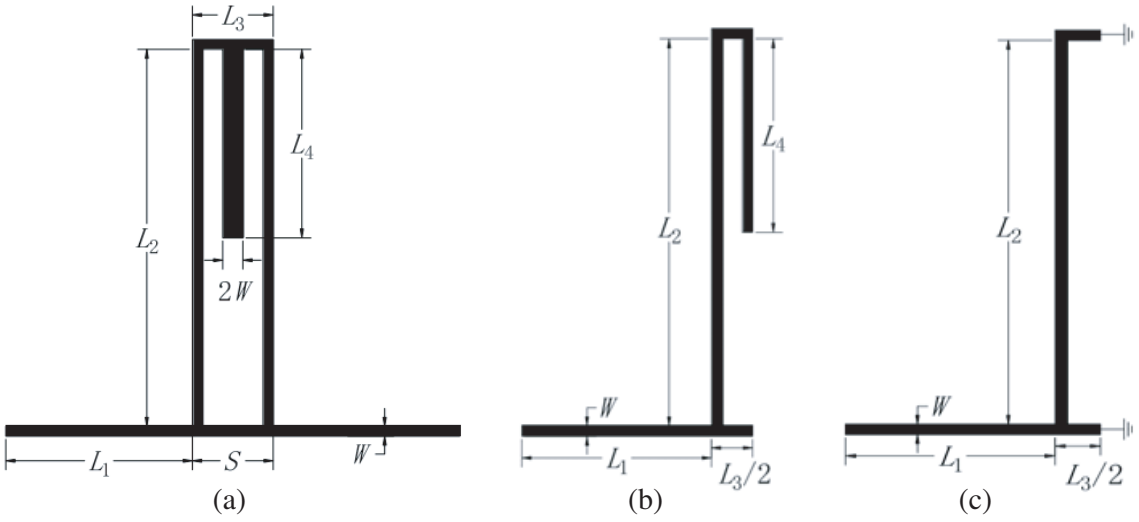

Figure 1. (a) Layout of square ring short stub loaded resonators. (b) Even-mode equivalent circuit. (c) Odd-mode equivalent circuit.

Figure 2 illustrates the EM simulated frequency responses of the above resonator under weak coupling with different dimension parameters of L_2 and L_3. In Fig. 2, four TZs (T_{Z1}, T_{Z2}, T_{Z3}, and T_{Z4}) and four transmission poles (T_{P1}, T_{P2}, T_{P3}, and T_{P4}) can be observed. According to (1) and (2), it can be deduced that T_{P1} and T_{P3} are the first and second even-order resonant frequency points. Meanwhile, T_{P2} and T_{P4} are the first and second odd-order resonant frequency points. T_{Z2} is derived from the out-of-phase cancellation of two signal paths. Fig. 2(a) and (b) show that T_{Z2} moves to lower frequency as L_2 changes from 7 to 7.5 and 8 mm, and L_3 varies from 1.2 to 1.6 and 2 mm, which can generate an adjustable notched-band under full wave simulation.

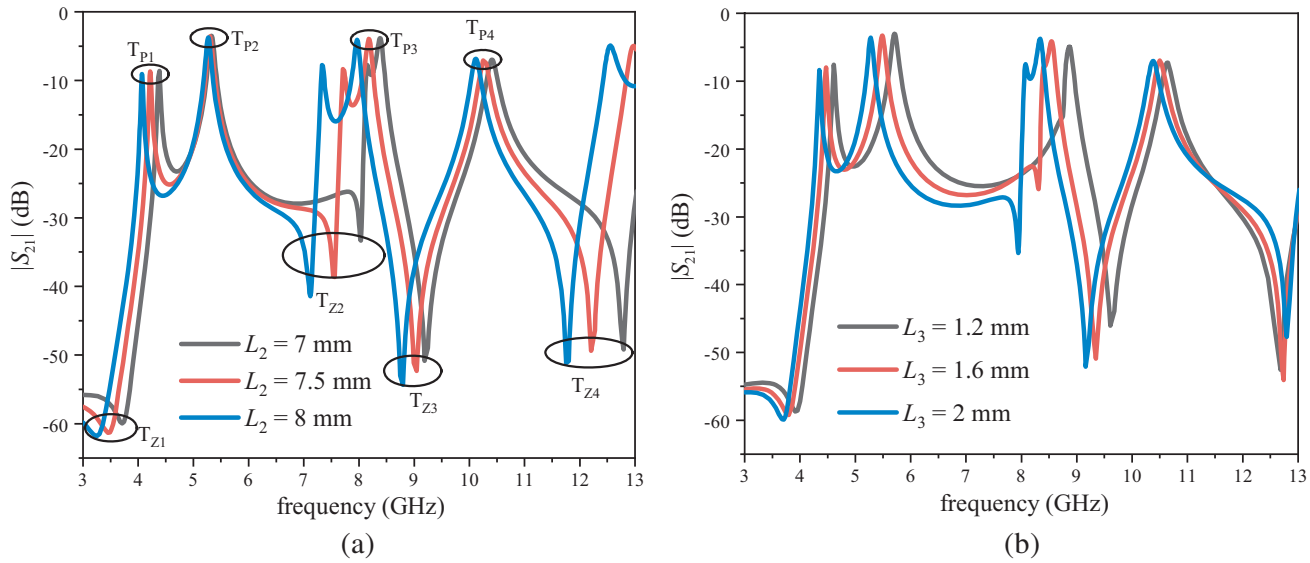

Figure 2. Simulated $|S_{21}|$ of the proposed resonator under weak coupling. Different L_2, L_3. (a) Different lengths L_2 when $L_1 = 4.5\,\text{mm}$, $L_3 = 1.9\,\text{mm}$, $L_4 = 3.3\,\text{mm}$, and $W = 0.2\,\text{mm}$. (b) Different lengths L_3 when $L_1 = 4.5\,\text{mm}$, $L_2 = 7\,\text{mm}$, $L_4 = 3.3\,\text{mm}$, and $W = 0.2\,\text{mm}$.

3. DESIGN AND RESULTS

Based on the characteristic analysis in the previous section, the structure is designed and debugged, as shown in Fig. 3(a). By adding two parallel coupled lines at both sides of the resonator in Fig. 3(a), a BPF with a notched-band is constructed, and its dimensions are $W_1 = 0.1\,\text{mm}$, $W_2 = W_3 = 0.2\,\text{mm}$, $W_4 = W_s = 0.4\,\text{mm}$, $L_1 = 3.7\,\text{mm}$, $L_2 = 7.7\,\text{mm}$, $L_4 = 3.8\,\text{mm}$, $gap_1 = 0.2\,\text{mm}$, and $gap_2 = 0.1\,\text{mm}$. The space of gap_1 denotes the coupling between source and load. The coupling is an electric coupling because the electric field is strong near the open end of the transmission lines. By similar reasoning, the space of gap_2 provides a coupling between I/O ports and the proposed resonator. The inclusion of the

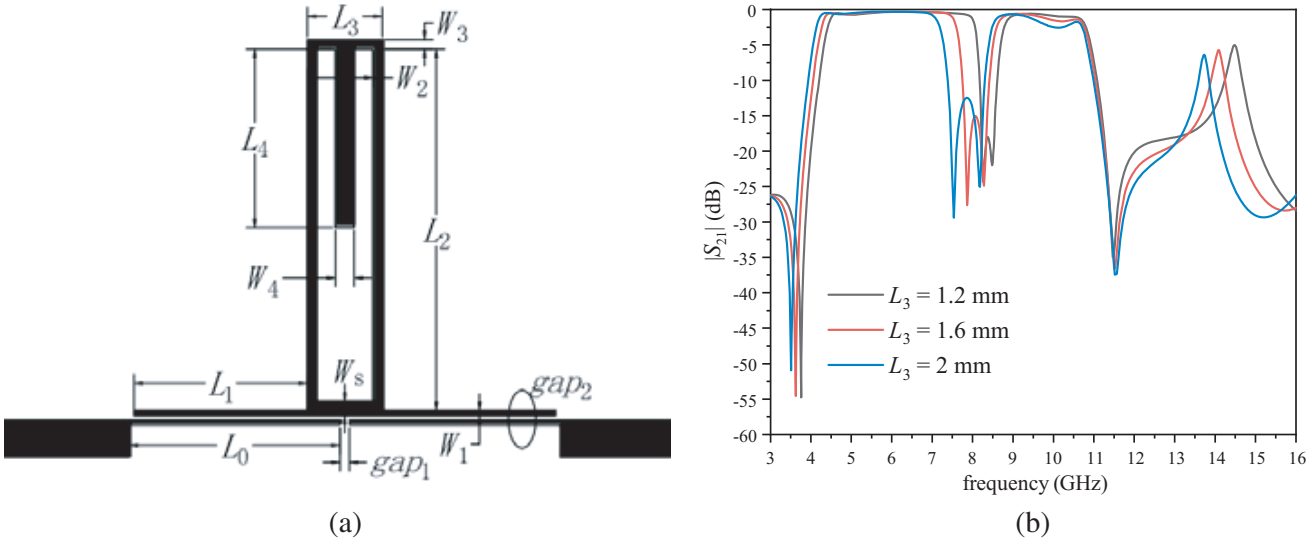

Figure 3. (a) Layout of the resonator using square ring with stepped impedance. (b) Simulated $|S_{21}|$ with different L_3.

two couplings may introduce two TZs at both sides of the passband [14]. In Fig. 3(b), the simulated results exhibit that the passband ranging from 4.2 ∼ 10.5 GHz appears, and the insertion loss of the stopband is higher than 15 dB. Furthermore, as L_3 is elongated, the resulting notched-band moves to lower frequency. This change does not significantly affect the overall passband performance. However, there is a harmonic passband around 14 GHz, which can affect out-band rejection of this filter. As illustrated in [15], an asymmetric loading stub can generate a TZ. So an L-shaped stub is introduced in the feeder position, as shown in Fig. 4(a). Fig. 4(b) is a photo of the fabricated filter, and Fig. 4(c) shows the simulated and measured frequency responses. It can be seen from Fig. 4(c) that the harmonic is suppressed around 14 GHz compared with Fig. 3(b). As previously described, a notched-band centered at 8.1 GHz appears due to out-of-phase cancellation of two signal paths. The notched-band can eliminate harmful interference of a satellite communication system. The high harmonic has disappeared, which can improve out-band rejection of this filter. Meanwhile, the presence of four TZs improves out-of-band rejection skirts in the passband. But the loss of measured results is significantly higher than that of simulated results. The visible difference between the measured and simulated results is caused by the inaccuracy of substrate properties and the deviation in the manufacturing process.

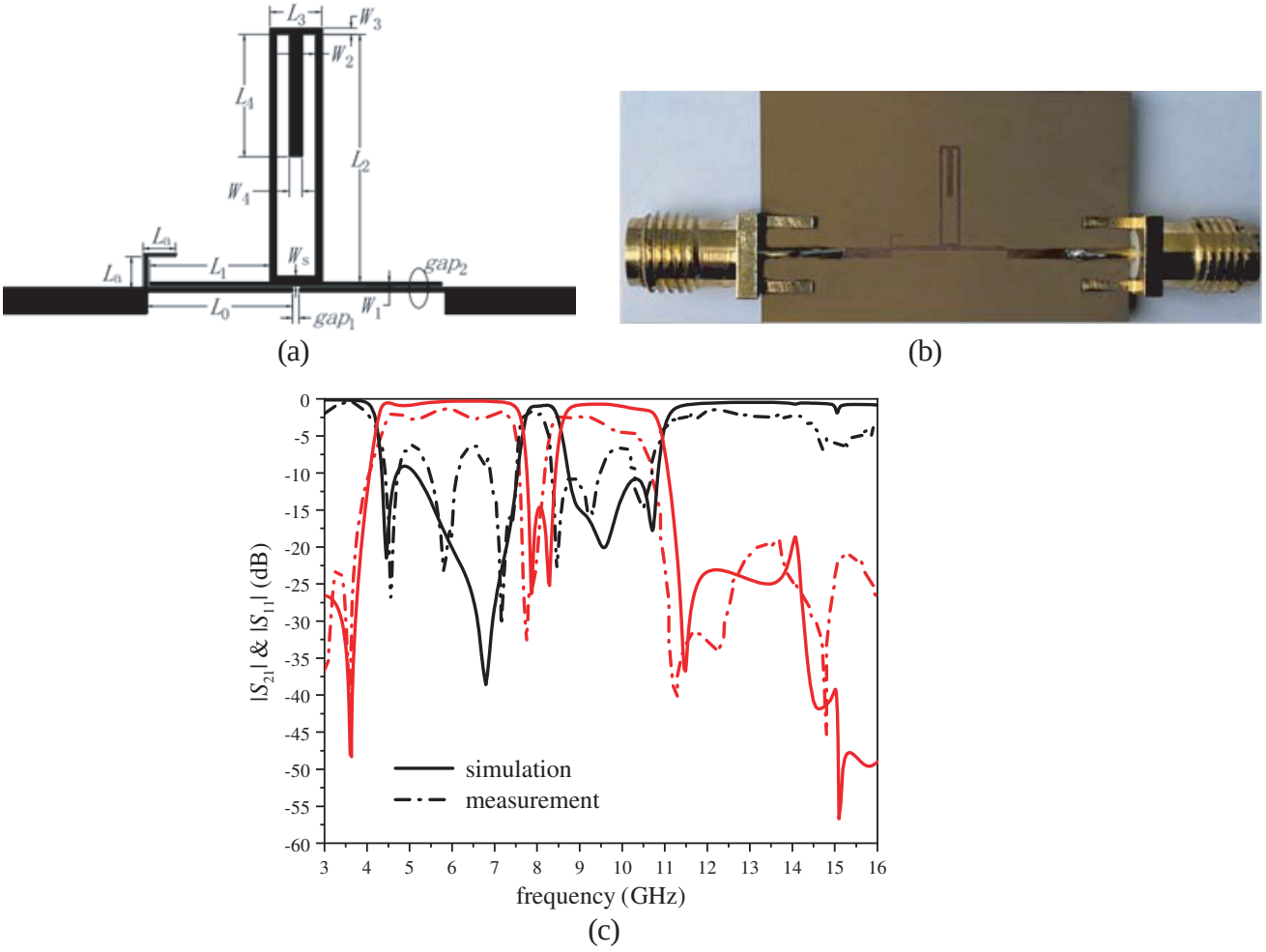

Figure 4. (a) Layout of the proposed filter. (b) Photo of the fabricated filter. (c) Simulated and measured results when $W_1 = 0.1$ mm, $W_2 = W_3 = 0.2$ mm, $W_4 = W_s = 0.4$ mm, $L_1 = 3.7$ mm, $L_2 = 7.7$ mm, $L_3 = 1.6$ mm, $L_4 = 3.8$ mm, $L_a = 1$ mm, $gap_1 = 0.2$ mm, and $gap_2 = 0.1$ mm.

4. CONCLUSION

This paper exhibits a method of a high-selective wideband bandpass filter with adjustable notched-band using square ring, and it is analyzed theoretically by using even- and odd-mode analysis. A uniform impedance resonator with an embedded open-circuited stub square loop can generate a wide passband with a notched-band. The structure can create four TZs, which make it have good out-of-band rejection skirts. Then, a TZ is created by introducing an open-circuited stub to input feed line, which can suppress higher harmonic passband around 14 GHz, and it can improve out-band rejection of the proposed filter. The proposed filter has a compact size. Finally, the proposed filter is fabricated and measured. The final simulated and measured results indicate that there is a wide passband with a notched-band centered at 8.1 GHz, and the proposed filter has advantages of good selectivity and stopband characteristics.

ACKNOWLEDGMENT

This work is supported in part by the Meritocracy Research Funds of China West Normal University under Grant 17YC054, Key projects of Sichuan Education Department under Grant 16ZA0172, and Study Abroad and Return Fund of China West Normal University under Grant 15B001.

REFERENCES

1. Yang, G. M., R. Jin, J. Geng, X. Huang, and G. Xiao, "Ultra-wideband bandpass filter with hybrid quasi-lumped elements and defected ground structure," *IET Microw. Antennas Propag.*, Vol. 1, No. 3, 733–736, 2007.
2. Basit, A., M. I. Khattak, and M. Al-Hasan, "Design and analysis of a microstrip planar UWB bandpass filter with triple notch bands for WiMAX, WLAN, and X-band satellite communication systems," *Progress In Electromagnetics Research M*, Vol. 93, 155–164, 2020.
3. Zhu, L., S. Sun, and W. Menzel, "Ultra-wideband (UWB) bandpass filters using multiple-mode resonator," *IEEE Microwave and Wireless Components Letters*, Vol. 15, No. 11, 796–798, 2005.
4. Zhang, S. and L. Zhu, "Compact and high-selectivity microstrip bandpass filters using triple-/quad-mode stub-loaded resonators," *IEEE Microwave and Wireless Components Letters*, Vol. 21, No. 10, 522–524, 2011.
5. Zhu, L. and W. Menzel, "Compact microstrip bandpass filter with two transmission zeros using a stub-tapped half-wavelength line resonator," *IEEE Microwave and Wireless Components Letters*, Vol. 13, Vol. 1, 16–18, 2003.
6. Ghazali, A. N. and S. Pal, "A compact UWB filter with notched band and suppressed stopband using DGS," *IETE Journal of Research*, Vol. 59, No. 4, 420–423, 2013.
7. Sengupta, A., S. Roychoudhury, and S. Das, "Design of a miniaturized multilayer tunable super wideband BPF," *Progress In Electromagnetics Research C*, Vol. 99, 145–156, 2020.
8. Chen, J. X., Y. L. Li, W. Qin, Y. J. Yang, and Z. H. Bao, "Compact multi-layer bandpass filter with wide stopband using selective feeding scheme," *IEEE Trans. Circuits Syst. II*, Vol. 65, 1009–1013, 2017.
9. Aliqab, K. and J. Hong, "UWB balanced BPF using a low-cost LCP bonded multilayer PCB technology," *IEEE Trans. Microw. Theory Tech.*, Vol. 67, No. 3, 1023–1029, 2019.
10. Mouavi, O., A. R. Eskandari, M. M. R. Kashani, and M. A. Shameli, "Compact UWB bandpass filter with two notched bands using SISLR and DMS structure," *Progress In Electromagnetics Research M*, Vol. 80, 193–201, 2019.
11. Liu, F. and M. Qun, "A new compact UWB bandpass filter with quad notched characteristics," *Progress In Electromagnetics Research Letters*, Vol. 88, 83–88, 2020.
12. Yang, L., W. W. Choi, K. W. Tam, and L. Zhu, "Novel wideband bandpass filter with dual notched bands using stub-loaded resonators," *IEEE Microwave and Wireless Components Letters*, Vol. 27, 25–27, 2017.

13. Guo, X., Y. Xu, and W. Wang, "Miniaturized planar ultra-wideband bandpass filter with notched band," *Journal of Computer and Communications*, Vol. 3, No. 3, 100–105, 2015.
14. Wang, C.-H., Y.-S. Lin, and C. H. Chen, "Novel inductance-incorporated microstrip coupled-line bandpass filters with two attenuation poles," *IEEE MTT-S Int. Microwave Symp. Dig.*, 1979–1982, 2004.
15. Shbman, H. and J.-S. Hong, "Asymmetric parallel-coupled lines for notch implementation in UWB filters," *IEEE Microwave and Wireless Components Letters*, Vol. 17, No. 7, 516–518, 2007.